



Research Article

Synthesis of CdTe Quantum Dots-based Imprinting Fluorescent Nanosensor for Highly Specific and Sensitive Determination of Caffeic Acid in Apple Juices

Ruiqing Long¹, Te Li^{1,2}, Lihui Wu¹, Shuyun Shi^{1,2,*}

¹College of Chemistry and Chemical Engineering, Central South University, Changsha 410083, P. R. China

²Key Laboratory of Human Province for Water Environment and Agriculture Product Safety, Central South University, Changsha 410083, P. R. China

ARTICLE INFO

Article History

Received 30 May 2019

Accepted 12 June 2019

Keywords

CdTe quantum dots
molecularly imprinted polymers
sol-gel polymerization
fluorescence detection
caffeic acid
apple juice

ABSTRACT

A facile method for the synthesis of molecularly imprinted polymers (MIPs) onto CdTe quantum dots (CdTe-QDs@MIPs) was successfully developed, and for the first time used as a sensitive fluorescent nanosensor for specific and rapid determination of caffeic acid (CA) in apple juices. Sol-gel polymerization was selected to fabricate hydrophilic MIPs layer using 3-(aminopropyl) triethoxysilane, tetraethyl orthosilicate, and CA as functional monomer, cross-linker and template, respectively. Under optimum experimental conditions, smaller CdTe-QDs@MIPs particles (48 nm) were synthesized with polymerization time at 2 min, which showed fast fluorescence quenching with response time at 3 min and high sensitivity with a limit of detection at 0.73 $\mu\text{g L}^{-1}$. The fluorescence intensity of CdTe-QDs@MIPs presented excellent linearity with the concentration of CA in the range from 2 to 100 $\mu\text{g L}^{-1}$ (R^2 , 0.9980). The developed method showed good repeatability with batch-to-batch relative standard deviation at 3.31%, and excellent selectivity over structural analogues. The practicability of the as-prepared CdTe-QDs@MIPs was confirmed by the analysis of CA in apple juices with satisfactory recoveries from 93.3% to 108.3%, and precisions <2.1%. Results demonstrated that a rapid, selective, and sensitive fluorescent method was successfully developed to detect CA in food samples.

© 2019 International Association of Dietetic Nutrition and Safety. Publishing services by Atlantis Press International B.V. This is an open access article distributed under the CC BY-NC 4.0 license (<http://creativecommons.org/licenses/by-nc/4.0/>)

1. INTRODUCTION

Caffeic acid (CA) is a phenolic acid and widely distributed in fruits, vegetables, and herbs, which plays a great role in our daily diet [1]. It is of great importance to quantitatively determine CA in our daily diet because of its antioxidant, anti-inflammatory, antibacterial, antitumor, immunomodulatory, and neuroprotective effects [2,3]. To date, several analytical methods have been developed to determine CA, such as high-performance liquid chromatography (HPLC) [4], gas chromatography [5], spectrophotometry [6], electrochemical [7], and fluorometric techniques [8,9]. Although these methods present good accuracy, high precision, and sensitivity, quantification of CA is still a challenging work because of the coexistence of phenolic components with similar structures in complex matrices, and some of the modern methods are laborious, expensive, complicated, and unsuitable for rapid and/or on-site analysis. So, development of easy-to-operate, low-cost, fast, sensitive, and selective methods for assessing CA in food samples are urgently needed.

Fluorescence methods have been recently widely explored for their simple, low-cost, and sensitive characteristics. Quantum dots (QDs) are considered as one of the new promising fluorescent materials,

which have been exploited in many analytical fields for the determination of various analytes due to their outstanding chemical and optical features over conventional organic fluorophores, such as facile preparation procedures, good aqueous dispersibility, superior chemical and photo stability, high photoluminescence efficiency, narrow symmetric emission profile, and excellent surface recognition ability [10,11]. Sun et al. [9] have synthesized carbon dots by the carbonization of urea and citric acid, and detected CA in red wine samples by fluorescence quenching process. Fan et al. [8] have investigated the interaction of CdTe quantum dots (CdTe-QDs) with CA and its structural similar compound, *p*-coumaric acid (pCA). The main limitation for the application of QDs-based fluorescence probes was their low selectivity; therefore, the surface of QDs should be modified by target-specific groups or materials to enhance specificity [8].

Molecularly imprinted polymers (MIPs) contain memory function of shape, size, and functional groups similar to template for high selectivity, which are then considered as an attractive strategy to modify the surface of QDs [12–16]. MIPs-based techniques have been developed for the selective extraction and determination of CA. Earlier, our group prepared CA-imprinted polymers as solid-phase extraction materials followed by HPLC detection [17,18]. Leite et al. [19] developed an MIPs film-based electrochemical sensor for selective determination of CA. Gültekin et al. [20] designed a CA-imprinted quartz crystal microbalance (QCM)

*Corresponding author. Email: shishuyun@126.com

Peer review under responsibility of the International Association of Dietetic Nutrition and Safety

nanosensor for selective quantification of CA. Recently, a report by Xu et al.'s [21] group covered carbon dots@MIPs for fluorescent determination of CA. MIPs are synthesized by different ways such as precipitation polymerization, bulk polymerization, suspension polymerization, and sol-gel polymerization [22–24]. It was noted that sol-gel polymerization is the most interesting method because of the simple synthesis process, water-compatible capability, and controllable particle size [25,26]. Suitable particle size of QDs@MIPs is critical to reduce the embedded recognition sites, and then gain favorable sensitivity and fast response rate [27].

In the current study, a facile and reliable fluorescence assay based on MIPs coated on the surface of CdTe-QDs (CdTe-QDs@MIPs) has been fabricated through sol-gel imprinting procedure for highly selective and sensitive determination of CA. Thioglycolic acid (TGA)-capped CdTe-QDs were produced, and then CdTe-QDs@MIPs were synthesized using 3-(aminopropyl)triethoxysilane (APTES), tetraethyl orthosilicate (TEOS), and CA as a functional monomer, cross-linker, and template, respectively. Relationships between polymerization time and particle size, fluorescence intensity, fluorescence quenching efficiency, equilibrium time, and limit of detection (LOD) for the detection of CA were exploited. The resultant CdTe-QDs@MIPs (polymerization time at 2 min, particle size at about 48 nm) were applied to detect CA in apple juices with equilibrium time within 3 min, and LOD at $0.73 \mu\text{g L}^{-1}$. Therefore, a rapid, selective, and sensitive method for the determination of CA was developed.

2. MATERIALS AND METHODS

2.1. Chemicals and Reagents

Tellurium powder, TGA, cadmium chloride ($\text{CdCl}_2 \cdot 2\text{H}_2\text{O}$), and sodium borohydride (NaBH_4) were bought from Aladdin Reagent Co., Ltd. (Shanghai, China). APTES, TEOS, anhydrous ethanol, sodium hydroxide (NaOH), and tris(hydroxymethyl)aminomethane (Tris-HCl) were purchased from Sinopharm Chemical Reagent Co., Ltd. (Shanghai, China). Standards, pCA, 4-hydroxybenzoic acid (4-HBA), vanillic acid (VA), ferulic acid (FA), CA, protocatechuic acid (PCA), and chlorogenic acid (CGA) were supplied by Xiya Reagent Co., Ltd. (Chengdu, China). All reagents were of analytical grade, used without any further treatment, and all stock solutions were prepared with ultrapure water ($18.2 \text{ M}\Omega$) from a Milli-Q water purification system (Millipore, Bedford, MA, USA).

2.2. Instrumentation

Fluorescence experiments were operated on an LS-55 fluorescence spectrometer (PerkinElmer Ltd., Washington, USA), and a Fluo Time 100 fluorescence spectrometer (PicoQuant, Germany). UV-Vis absorption spectra were accomplished on a UV-2600 spectrometer (Shimadzu, Tokyo, Japan). A Nicolet-Avatar 360 Fourier transform infrared (FTIR) spectrometer within the wavenumber from 400 to 4000 cm^{-1} was selected to study the functional groups. The size, structure, and morphology of CdTe-QDs@MIPs were carried out on a Tecnai G2 20S-Twin transmission electron microscope (TEM, FEI, Prague, Czech Republic). The average values of the particle size and polydispersity of microspheres were acquired on a particle size analysis (PSA) (Malvern Instruments Ltd., Malvern, UK), and 100 particles were used in the analysis process.

High-performance liquid chromatography analysis was operated on an Agilent 1260 HPLC system (Agilent Technologies, Santa Clara, CA, USA). Apple juice samples were separated on a Waters SunFire-C₁₈ chromatographic column ($250 \times 4.6 \text{ mm}^2 \text{ i.d.}$, $5 \mu\text{m}$, Waters, Milford, MA, USA). Mobile phase consisting of 0.1% acetic acid/acetonitrile (85/15, v/v) was isocratic eluted with a flow rate of 0.8 mL min^{-1} . Detection wavelength was set at 325 nm, column temperature was at 25°C , and injection volume was $20 \mu\text{L}$.

2.3. Synthesis of CdTe-QDs@MIPs

The schematic illustration for fabrication of CdTe-QDs@MIPs was presented in Figure S1. First, TGA-capped CdTe-QDs were synthesized using a method modified from an earlier report [27]. In detail, 30.7 mg of $\text{CdCl}_2 \cdot 2\text{H}_2\text{O}$ and $70 \mu\text{L}$ of TGA were dissolved in 100 mL of water, and subsequently 0.5 mol L^{-1} of NaOH solution was selected to adjust pH to 9.0. Simultaneously, 25.5 mg of tellurium powder and 30.3 mg of NaBH_4 were mixed in 2.0 mL of water, and continuously stirred under nitrogen atmosphere for 3 h to prepare NaHTe solution. The abovementioned two solutions were then rapidly blended and refluxed at 90°C for 13 h to obtain TGA-capped CdTe-QDs solution. For the synthesis of CdTe-QDs@MIPs, sol-gel polymerization was used. Briefly, 0.5 mg of CA, 4 mL of ethanol, 1 mL of H_2O , and $20 \mu\text{L}$ of APTES were mixed and stirred at room temperature for 30 min. After that, 10 mL of TGA-capped CdTe-QDs solution and $10 \mu\text{L}$ of TEOS were added and continuously stirred for 1, 2, 3, 5, 10, or 15 min. Mixtures were centrifuged at 9000 rpm for 1 min. The resultant precipitate was washed with ethanol to remove CA until no CA was detected by UV-Vis spectrometry. Correspondingly, CdTe-QDs@non-imprinted polymers (CdTe-QDs@NIPs) were prepared with the same procedures as described for CdTe-QDs@MIPs in the absence of CA. Finally, the resultant CdTe-QDs@MIPs and CdTe-QDs@NIPs were dried under vacuum for 1 h and kept in a refrigerator at 4°C for subsequent experiments.

2.4. Fluorescence Measurements

Fluorescence spectroscopy was acquired under the same conditions, excitation wavelength at 380 nm, excitation and emission slit width at 10 nm, photomultiplier tube voltage at 900 V, and spectral range at 550–650 nm. For determination of CA, 0.3 mL of CdTe-QDs@MIPs or CdTe-QDs@NIPs solution (0.1 mg mL^{-1}), 2.7 mL of Tris-HCl buffer (10 mM, pH 8.0), and $30 \mu\text{L}$ of CA standard solution (0 – 10.0 mg L^{-1}) were mixed and incubated for 3 min at room temperature to record fluorescence spectra, and fluorescence intensities were recorded at 600 nm. Experiments were conducted in triplicate to calculate average data.

2.5. Determination of CA in Apple Juices

Two brands of apple juices (Huiyuan apple juice, Beijing Huiyuan Beverage and Food Co., Ltd., China; Huiyuan apple juice, Xiameng Huiyuan Food Co., Ltd., China) were bought from the local supermarket in Changsha. Apple juices were filtered through a $0.22 \mu\text{m}$ polytetrafluoroethylene syringe filter, and then, $30 \mu\text{L}$ of apple juices, 0.3 mL of CdTe-QDs@MIPs solution, and 2.7 mL of Tris-HCl buffer (10 mM, pH 8.0) were mixed, incubated for 3 min, and then detected.

3. RESULTS AND DISCUSSION

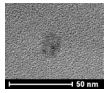
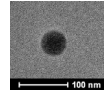
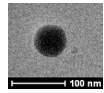
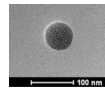
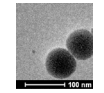
3.1. Synthesis and Characterization of CdTe-QDs@MIPs

As is shown in Figure S1, surface MIPs are synthesized by sol-gel polymerization. The pK_{a1} and pK_{a2} values of CA are 4.49 and 7.64, and that of APTES is around 9.6. Therefore, at neutral condition, carboxyl group in CA is deprotonated, and the amino group in APTES can interact with hydroxyl and carboxyl groups in CA through electrostatic interaction and hydrogen bonds to form prepolymerization complex, and then hydrolysis and condensation reactions of APTES and TEOS happen to imprint CA in the composites. After the removal of CA, recognition sites are formed. As presented in Table 1, particle size increases with the increase of polymerization time. Figure 1 presents the morphology and particle size of CdTe-QDs@MIPs when the

polymerization time is 2 min, which presents monodisperse particles with an average diameter of 48 nm, and high amounts of CdTe-QDs are uniformly trapped into MIPs layer. The maximum emission of CdTe-QDs@MIPs is about 600 nm when excited at 380 nm, the fluorescence intensity of CdTe-QDs@MIPs after the addition of CA is relatively weak, and restores to 93.0% that of CdTe-QDs@NIPs (Figure S2). These results indicate that CdTe-QDs@MIPs with CA recognition have been successfully synthesized, and template CA has been almost removed from the recognition sites.

Molar ratio of template-functional monomer-crosslinker is important to affect the recognition ability of MIPs [17]. CdTe-QDs@MIPs with different ratios of CA:APTES:TEOS (1:17:16–1:85:16) have been prepared, and the maximum fluorescence intensity and highest quenching efficiency by the addition of CA are obtained when the molar ratio of CA:APTES:TEOS is at 1:34:16 (Figure 2A). Moreover, appropriate particle size must be controlled to reduce

Table 1 Effects of polymerization time on the particle size, incubation time, and LOD of CdTe-QDs@MIPs for detection of CA

Polymerization time (min)	1	2	3	5	10	15
TEM						
Average particle size (nm)	15	48	55	59	65	70
Incubation time (min)	3	3	5	7	10	12
LOD ($\mu\text{g L}^{-1}$)	0.89	0.73	0.95	2.53	3.25	3.56

LOD, limit of detection; CA, caffeic acid; TEM, transmission electron microscope.

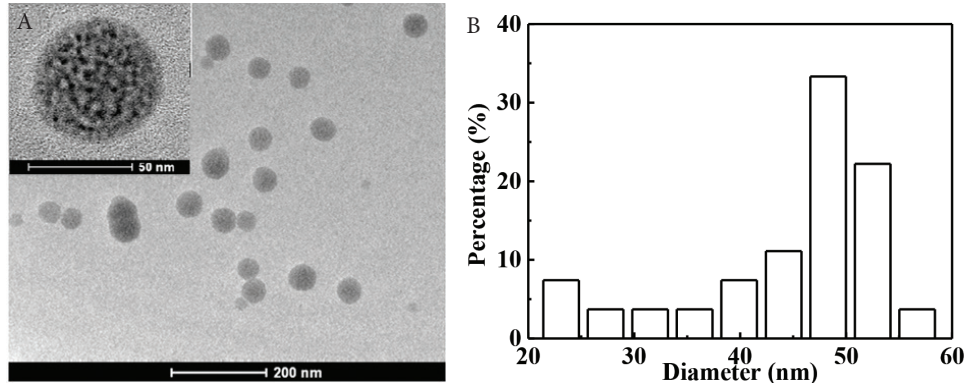


Figure 1 | TEM image (50 nm for the inset) (A) and PSA histogram (B) of CdTe-QDs@MIPs with polymerization time at 2 min. PSA, particle size analysis.

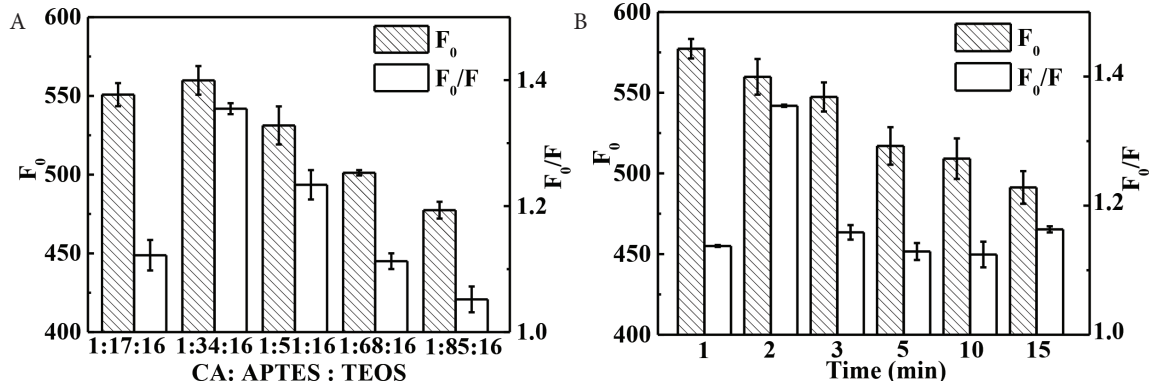


Figure 2 | Effect of the ratio of CA:APTES:TEOS (A) and polymerization time (B) on the fluorescence response and quenching efficiency of CdTe-QDs@MIPs (concentration of CA at $10 \mu\text{g L}^{-1}$). CA, caffeic acid; APTES, 3-(aminopropyl)triethoxysilane; TEOS, tetraethyl orthosilicate; QD, quantum dot; MIP, molecularly imprinted polymer.

embedded recognition sites, and provide high binding efficiency [26]. As is shown in Figure 2B, fluorescence intensity of CdTe-QDs@MIPs decreases with the increase of polymerization time perhaps because of the deeper embedded CdTe-QDs and recognition sites, and the highest quenching efficiency of CA presents with polymerization time at 2 min.

Fourier transform infrared spectra has been used to characterize CdTe-QDs@MIPs (Figure 3). The main absorption bands for TGA-modified CdTe-QDs are located at 1211 cm^{-1} (O—H stretching), 1403 cm^{-1} (C=O stretching), and 1581 cm^{-1} (deformation vibration of carboxylic group), respectively (Figure 3A). Also, for

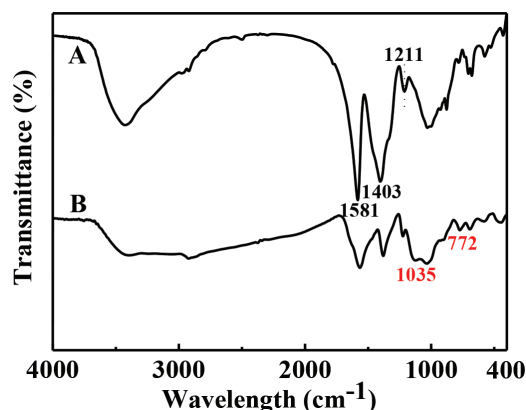


Figure 3 | FTIR spectra of TGA-capped CdTe-QDs (A), and CdTe-QDs@MIPs (B). FTIR, Fourier transform infrared; TGA, thioglycolic acid; QD, quantum dot; MIP, molecularly imprinted polymer.

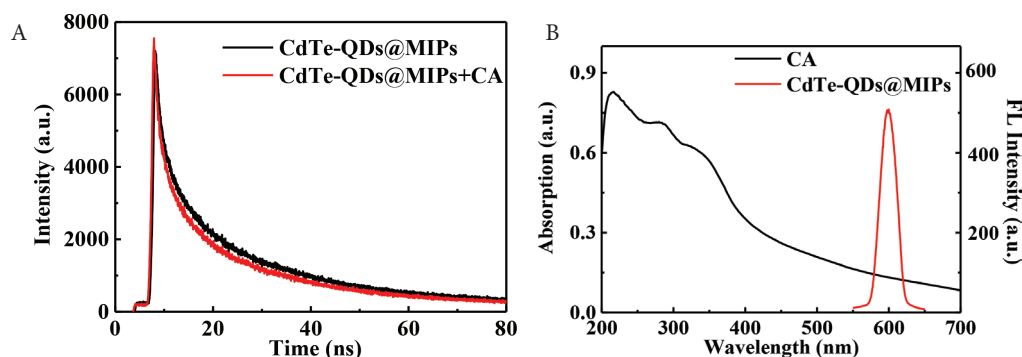


Figure 4 | Fluorescence lifetime spectra of CdTe-QDs@MIPs in the absence and presence of CA (A). UV-Vis absorption spectrum of CA and fluorescence emission spectrum of CdTe-QDs@MIPs (B). CA, caffeic acid; QD, quantum dot; MIP, molecularly imprinted polymer.

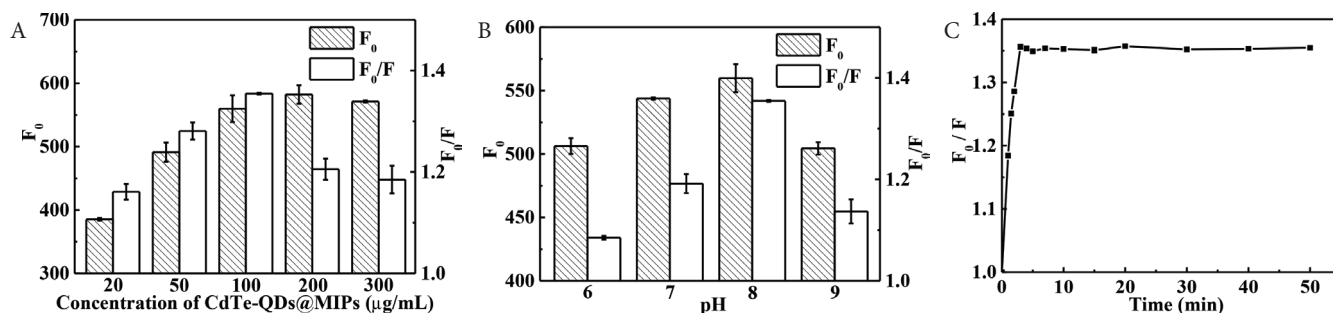


Figure 5 | Effect of the amount of CdTe-QDs@MIPs (A), pH (B), and incubation time (C) on the response of CdTe-QDs@MIPs to CA (concentration of CA at $10\text{ }\mu\text{g L}^{-1}$). CA, caffeic acid; QD, quantum dot; MIP, molecularly imprinted polymer.

CdTe-QDs@MIPs, the specific peaks at 1035 cm^{-1} (asymmetric stretching of Si—O—Si) and 772 cm^{-1} (bending vibration of Si—O) indicate successful sol-gel polymerization (Figure 3B).

3.2. Sensing Mechanism of CdTe-QDs@MIPs

As is shown in Figure 4A, fluorescence lifetime of CdTe-QDs@MIPs is $15.56 \pm 0.94\text{ ns}$, which reduces to $12.28 \pm 0.77\text{ ns}$ after the addition of CA. The reduced fluorescence lifetime suggests that energy or charge transfer should happen between CdTe-QDs and CA [28]. Maximum adsorption bands for CA are 254 and 326 nm, which are close to the band gap of CdTe-QDs [27], and far away from the emission spectrum (600 nm) of CdTe-QDs@MIPs (Figure 4B). Therefore, charges in the conduction band of CdTe-QDs can transfer to the lowest unoccupied molecular orbital of CA, and energy resonance transfer is not the possible quenching mechanism. Furthermore, hydroxyl and carboxyl groups in CA can interact with amino group in APTES through electrostatic interaction and hydrogen bond; therefore, it is concluded that the observed fluorescence quenching is attributed to the charge transfer between CA and CdTe-QDs.

3.3. Optimization of Determination Conditions for CA

The main factors, such as the amount of CdTe-QDs@MIPs, pH, and response time, affecting the fluorescence intensity and quenching efficiency have been optimized to improve sensitivity. Different amounts of CdTe-QDs@MIPs has been first investigated. Figure 5A

indicates that fluorescence intensity increases with the increase in CdTe-QDs@MIPs concentrations from 20 to 100 $\mu\text{g mL}^{-1}$, then provides no significant difference from 100 to 300 $\mu\text{g mL}^{-1}$, and the highest quenching efficiency is achieved with CdTe-QDs@MIPs concentration at 100 $\mu\text{g mL}^{-1}$. Lower CdTe-QDs@MIPs concentration results in lower fluorescence intensity and narrow linear range, whereas higher CdTe-QDs@MIPs concentration reduces slight agglomeration and then results in low sensitivity [29]. Therefore, CdTe-QDs@MIPs concentration has been optimized as 100 $\mu\text{g mL}^{-1}$. pH from 6.0 to 9.0 has done to investigate the effect of pH (Figure 5B). Fluorescence intensity of CdTe-QDs@MIPs and quenching efficiency after the addition of CA increases by increasing the pH from 6.0 to 8.0, and then decreases from 8.0 to 9.0. Accordingly, 8.0 has been chosen as the best pH value. A certain time is required to allow an efficient recognition interaction between CA and CdTe-QDs@MIPs. As illustrated in Figure 5C, quenching efficiency of CdTe-QDs@MIPs increases sharply at first, and then shows stabilizes after 3 min incubation. Therefore, incubation time has been set at 3 min, which indicates that CdTe-QDs@MIPs can be used to rapidly detect CA in aqueous solution. Earlier, the incubation time for QDs@MIPs with particle size over 200 nm (polycondensation time from 6 to 16 h) was 30–60 min [27]. From Table 1, we can also see that incubation times are 3, 3, 5, 7, 10, and 12 min for CdTe-QDs@MIPs with polymerization time at 1, 2, 3, 5, 10, and 15 min. The fast mass transfer rate is assigned to CdTe-QDs@MIPs with smaller particle size where recognition sites is easily entered for binding.

3.4. Specificity and Stability Study

Six structural analogues (FA, CGA, pCA, VA, 4-HBA, and PCA) with concentration at 10 $\mu\text{g L}^{-1}$ have been used to investigate their fluorescence response to CdTe-QDs@MIPs and CdTe-QDs@NIPs. As is shown in Figure 6, the quenching efficiency of CA to CdTe-QDs@MIPs (F_0/F , 1.35) is much higher than that for CdTe-QDs@NIPs (F_0/F , 1.03), which verifies that CdTe-QDs@MIPs have imprinted cavities for specific recognition of CA. Furthermore, no significant differences of quenching efficiencies (all close to 1.00) have been observed among FA, CGA, pCA, VA, 4-HBA, and PCA to CdTe-QDs@MIPs and CdTe-QDs@NIPs because of the absence of tailor-made recognition sites.

The stability of CdTe-QDs@MIPs in an aqueous solution at 4°C has been evaluated over a period of 12 weeks. As presented in Figure S3, no discernible changes are found during the first 6 weeks, as the fluorescence intensity retains 97.61% of its initial fluorescence response. In addition, five batches of CdTe-QDs@MIPs have been prepared, and batch-to-batch relative standard deviation (RSD) is 3.31%, probably because MIPs shell plays an important role in the protection of CdTe-QDs@MIPs from self-fluorescence quenching effect.

3.5. Analytical Figures for the Determination of CA

Under the optimized experimental conditions, fluorescence intensities of CdTe-QDs@MIPs and CdTe-QDs@NIPs have been investigated by addition of different concentrations of CA from 0 to 100 $\mu\text{g L}^{-1}$ to evaluate their analytical performances, such as linearity, LOD ($3\sigma/k$), limit of quantification (LOQ, $10\sigma/k$), precision, and specificity. As is depicted in Figure 7, fluorescence intensities of CdTe-QDs@MIPs apparently decrease with the increase of CA concentrations, and that for CdTe-QDs@NIPs is not obvious. Fluorescence quenching efficiencies can be depicted by Stern–Volmer type equation: $F_0/F = 1 + K_{sv}[C]$, where K_{sv} and $[C]$ are

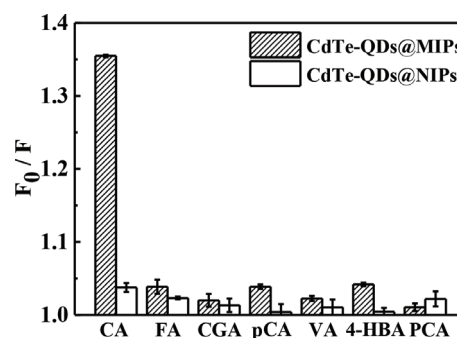


Figure 6 | Quenching efficiencies of CA, FA, CGA, pCA, VA, 4-HBA, and PCA (each concentration at 10 $\mu\text{g L}^{-1}$) on CdTe-QDs@MIPs and CdTe-QDs@NIPs. CA, caffeic acid; FA, ferulic acid; CGA, chlorogenic acid; pCA, *p*-coumaric acid; VA, vanillic acid; HBA, hydroxybenzoic acid; PCA, protocatechuic acid; QD, quantum dot; MIP, molecularly imprinted polymer; NIP, non-imprinted polymer.

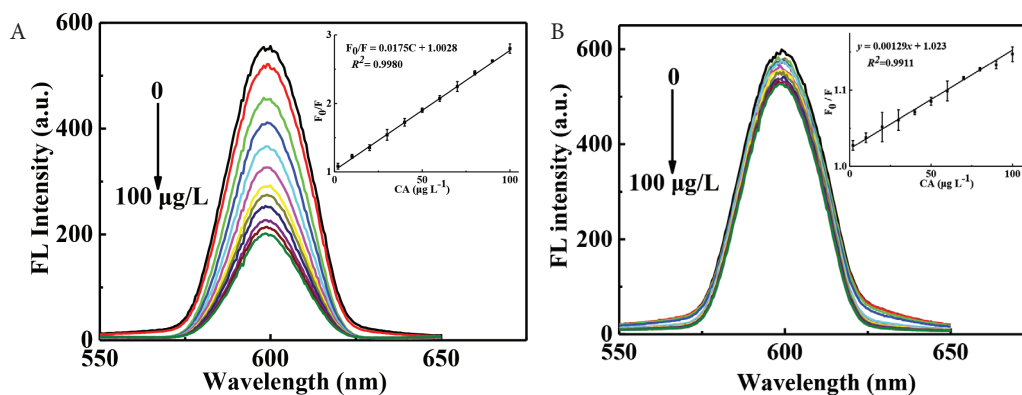


Figure 7 | Fluorescence spectra of CdTe-QDs@MIPs (A) and CdTe-QDs@NIPs (B) on addition of different concentrations of CA (0–100 $\mu\text{g L}^{-1}$), inset was the calibration graph. CA, caffeic acid; QD, quantum dot; MIP, molecularly imprinted polymer; NIP, non-imprinted polymer.

Table 2 | Comparison of the developed method with other reported methods for CA determination

Detection scheme	Real sample	Linear range ($\mu\text{g L}^{-1}$)	LOD ($\mu\text{g L}^{-1}$)	Reference
HPLC-electrochemical detector	Honeysuckle	50–1.0 $\times 10^4$	1.6	Ye et al. [4]
Au electrode@MIPs	Wines	90–1.1 $\times 10^4$	27.0	Leite et al. [19]
Electrochemical method	Plasma	4.5 $\times 10^3$ –3.6 $\times 10^5$	901.5	Valentini et al. [7]
QCM@MIPs	Plant materials	1.8–1.8 $\times 10^5$	1.4	Gültekin et al. [20]
MIPs–HPLC	Fruits	1.0 $\times 10^3$ –1.0 $\times 10^5$	200	Fan et al. [18]
CdTe-QDs	–	667.8–2.0 $\times 10^4$	216	Fan et al. [8]
Carbon dots	Red wine	140–1.8 $\times 10^4$	43.2	Sun et al. [9]
Carbon dots@MIPs	Plasma	90.1–3.6 $\times 10^4$	19.8	Xu et al. [21]
CdTe-QDs@MIPs	Apple juices	2.0–100.0	0.73	This work

CA, caffeic acid; HPLC, high-performance liquid chromatography; MIP, molecularly imprinted polymer; QCM, quartz crystal microbalance; QD, quantum dot.

Table 3 | Recoveries of CA in apple juices (diluted 100-fold) by CdTe-QDs@MIPs based sensor ($n = 3$)

Sample	Added ($\mu\text{g L}^{-1}$)	Found ^a ($\mu\text{g L}^{-1}$)	Recovery (%)	RSD (%)
Huiyuan	0	11.80	– ^b	3.95
apple	5.0	17.14	106.7	0.55
juice	20.0	32.14	101.7	2.10
	50.0	59.45	95.3	0.76
Huierkang	0	9.92	– ^b	5.30
apple	5.0	14.59	93.3	0.70
juice	20.0	31.58	108.3	1.78
	50.0	56.92	94.0	1.90

^aMean of three determinations, ^bNot detected.

the quenching constant and concentration of CA, respectively. As is shown in the inset of Figure 7, K_{sv} for CdTe-QDs@MIPs is considerably larger than that for CdTe-QDs@NIPs, and the ratio of K_{sv} values (i.e., imprinting factor) is 13.6, which also indicates the presence of specific recognition sites on CdTe-QDs@MIPs. Good linearity ($F_0/F = 1.0028 + 0.0175C$) with wide linear range (2–100 $\mu\text{g L}^{-1}$) and high coefficient ($R^2 = 0.9980$) has been obtained for CA by CdTe-QDs@MIPs. Based on the results, LOD (0.73 $\mu\text{g L}^{-1}$) and LOQ (2.40 $\mu\text{g L}^{-1}$) have been achieved for CA. In comparison, LOD (0.89, 0.95, 2.53, 3.25, and 3.56 $\mu\text{g L}^{-1}$) has been calculated for CA detection by CdTe-QDs@MIPs with polymerization time for 1, 3, 5, 10, and 15 min, respectively (Table 1). Therefore, smaller particle size with appropriate recognition sites result in higher sensitivity detection. Intra-day RSD value at 1.3% indicates the high reproducibility, and the inter-day RSD value at 6.4% over a 6-day span also presents the small signal variability. Accordingly, the developed method is sufficiently practical for the quantification of CA. Compared with previously reported quantitative methods for CA [4,7–9,18–21] (Table 2), the developed method demonstrates higher sensitivity.

3.6. Real Sample Measurement

The practical feasibility of this CdTe-QDs@MIPs fluorescence sensor has been evaluated for the quantitative analysis of CA in apple juices. Samples were just diluted 100-fold without any additional pretreatment procedures. The recoveries of CA range from 93.3% to 108.3% with excellent RSD values <2.10% (Table 3), which suggests that the proposed method is sufficiently accurate for selective determination of CA. Finally, CA has been estimated in Huiyuan apple juice and Huierkang apple juice at concentrations of 1180 ± 47 and $992 \pm 53 \mu\text{g L}^{-1}$, respectively.

In the Pharmacopoeia of the People's Republic of China, CA is always quantified by HPLC–UV. Then, the quantitative analysis of CA in Huiyuan apple juice and Huierkang apple juice has been proposed to be performed using HPLC–UV as reported in our earlier studies [17,18] (see Figure S4). Results indicate the concentrations of CA in Huiyuan apple juice and Huierkang apple juice are 1150 ± 41 and $1080 \pm 60 \mu\text{g L}^{-1}$, which is in consistency with those determined by our developed CdTe-QDs@MIPs-based method.

4. CONCLUSION

In this work, we have fabricated a facile synthesis of CdTe-QDs@MIPs for rapid, sensitive, and selective determination of CA in apple juices for the first time. CdTe-QDs@MIPs can be simply synthesized by anchoring MIPs layer on the surface of CdTe-QDs via sol–gel polymerization. Combining the selectivity of MIPs with the sensitivity of CdTe-QDs, CdTe-QDs@MIPs present overwhelming properties. Small particle size with appropriate recognition sites largely shortens the response time and improves sensitivity. The excellent properties of CdTe-QDs@MIPs have revealed their great potentials in advanced analytical applications.

CONFLICTS OF INTEREST

The authors declare they have no conflicts of interest.

AUTHORS' CONTRIBUTION

RL contributed in data curation, and writing–original draft. RL and TL contributed in formal analysis and investigation. RL and LW contributed in methodology and validation. RL and SS contributed in supervision. SS contributed in funding acquisition, project administration and writing–review & editing.

ACKNOWLEDGMENTS

The authors acknowledge the financial support of the National Natural Science Foundation of China (31660181), Provincial Natural Science Foundation of Hunan (2018JJ1043), and Key Laboratory of Hunan Province for Water Environment and Agriculture Product Safety (2018TP1003).

REFERENCES

- [1] Wang G, Lei Z, Zhong Q, Wu W, Zhang H, Min T, et al. Enrichment of caffeic acid in peanut sprouts and evaluation of its *in vitro* effectiveness against oxidative stress-induced erythrocyte hemolysis. *Food Chem* 2017;217:332–41.
- [2] Cid A, Moldes OA, Mejuto JC, Simal-Gandara J. Interaction of caffeic acid with SDS micellar aggregates. *Molecules* 2019;24: pii: E1204.
- [3] Wang GF, Shi LP, Ren YD, Liu QF, Liu HF, Zhang RJ, et al. Anti-hepatitis B virus activity of chlorogenic acid, quinic acid and caffeic acid *in vivo* and *in vitro*. *Antiviral Res* 2009;83:186–90.
- [4] Ye LH, Du LJ, Cao J. Fatty acids-based microemulsion liquid chromatographic determination of multiple caffeoylquinic acid isomers and caffeic acid in honeysuckle sample. *J Pharm Biomed Anal* 2019;171:22–9.
- [5] Jung MY, Lee DE, Cheng HY, Chung IM, Kim SH, Han JG, et al. Characterization of volatile profiles of six popular edible mushrooms using headspace-solid-phase microextraction coupled with gas chromatography combined with chemometric analysis. *J Food Sci* 2019;84:421–9.
- [6] Robbins RJ. Phenolic acids in foods: an overview of analytical methodology. *J Agric Food Chem* 2003;51:2866–87.
- [7] Valentini F, Roscioli D, Carbone M, Conte V, Floris B, Bauer EM, et al. Graphene and ionic liquids new gel paste electrodes for caffeic acid quantification. *Sens Actuators B* 2015;212:248–55.
- [8] Fan X, Liu S, He Y. Study on the interaction of CdTe quantum dots with coumaric acid and caffeic acid based on fluorescence reversible tune. *Colloids Surf B Biointerfaces* 2011;88:23–30.
- [9] Sun Q, Long Y, Li H, Pan S, Yang J, Liu S, et al. Fluorescent carbon dots as cost-effective and facile probes for caffeic acid sensing via a fluorescence quenching process. *J Fluoresc* 2018;28:523–31.
- [10] Foubert A, Beloglazova NV, Rajkovic A, Sas B, Madder A, Goryacheva IY, et al. Bioconjugation of quantum dots: Review & impact on future application. *TrAC Trends Anal Chem* 2016;83:31–48.
- [11] Molaei MJ. A review on nanostructured carbon quantum dots and their applications in biotechnology, sensors, and chemiluminescence. *Talanta* 2019;196:456–78.
- [12] Ahmadpour H, Hosseini SMM. A solid-phase luminescence sensor based on molecularly imprinted polymer-CdSeS/ZnS quantum dots for selective extraction and detection of sulfasalazine in biological samples. *Talanta* 2019;194:534–41.
- [13] Chen L, Wang X, Lu W, Wu X, Li J. Molecular imprinting: perspectives and applications. *Chem Soc Rev* 2016;45:2137–211.
- [14] Chmangui A, Driss MR, Touil S, Bermejo-Barrera P, Bouabdallah S, Moreda-Piñeiro A. Aflatoxins screening in non-dairy beverages by Mn-doped ZnS quantum dots – molecularly imprinted polymer fluorescent probe. *Talanta* 2019;199:65–71.
- [15] Li J, Fu J, Yang Q, Wang L, Wang X, Chen L. Thermosensitive molecularly imprinted core-shell CdTe quantum dots as a ratiometric fluorescence nanosensor for phycocyanin recognition and detection in seawater. *Analyst* 2018;143:3570–8.
- [16] Yang Q, Li J, Wang X, Peng H, Xiong H, Chen L. Strategies of molecular imprinting-based fluorescence sensors for chemical and biological analysis. *Biosens Bioelectron* 2018;112:54–71.
- [17] Fan D, Li H, Shi S, Chen X. Hollow molecular imprinted polymers towards rapid, effective and selective extraction of caffeic acid from fruits. *J Chromatogr A* 2016;1470:27–32.
- [18] Fan D, Jia L, Xiang H, Peng M, Li H, Shi S. Synthesis and characterization of hollow porous molecular imprinted polymers for the selective extraction and determination of caffeic acid in fruit samples. *Food Chem* 2017;224:32–6.
- [19] Leite FRF, Santos WDJR, Kubota LT. Selective determination of caffeic acid in wines with electrochemical sensor based on molecularly imprinted siloxanes. *Sens Actuators B* 2014;193:238–46.
- [20] Gültekin A, Karanfil G, Kuş M, Sönmezoğlu S, Say R. Preparation of MIP-based QCM nanosensor for detection of caffeic acid. *Talanta* 2014;119:533–7.
- [21] Xu X, Xu G, Wei F, Cen Y, Shi M, Cheng X, et al. Carbon dots coated with molecularly imprinted polymers: a facile bioprobe for fluorescent determination of caffeic acid. *J Colloid Interface Sci* 2018;529:568–74.
- [22] Ji W, Wang R, Mu Y, Wang X. Superhydrophilic molecularly imprinted polymers based on a single cross-linking monomer for the recognition of iridoid glycosides in *Di-huang* pills. *Anal Bioanal Chem* 2018;410:6539–48.
- [23] Li H, Long R, Tong C, Li T, Liu Y, Shi S. Shell thickness controlled hydrophilic magnetic molecularly imprinted resins for high-efficient extraction of benzoic acids in aqueous samples. *Talanta* 2019;194:969–76.
- [24] Zhou T, Ding L, Che G, Jiang W, Sang L. Recent advances and trends of molecularly imprinted polymers for specific recognition in aqueous matrix: preparation and application in sample pretreatment. *Trends Anal Chem* 2019;114:11–28.
- [25] Bie Z, Chen Y, Ye J, Wang S, Liu Z. Boronate-affinity glycan-oriented surface imprinting: a new strategy to mimic lectins for the recognition of an intact glycoprotein and its characteristic fragments. *Angew Chem Int Ed Engl* 2015;54:10211–5.
- [26] Peng M, Xiang H, Hu X, Shi S, Chen X. Boronate affinity-based surface molecularly imprinted polymers using glucose as fragment template for excellent recognition of glucosides. *J Chromatogr A* 2016;1474:8–13.
- [27] Chullasat K, Nurerk P, Kanatharana P, Davis F, Bunkoed O. A facile optosensing protocol based on molecularly imprinted polymer coated on CdTe quantum dots for highly sensitive and selective amoxicillin detection. *Sens Actuators B* 2018;254:255–63.
- [28] Huang S, Wang L, Zhu F, Su W, Sheng J, Huang C, et al. A ratiometric nanosensor based on fluorescent carbon dots for label-free and highly selective recognition of DNA. *RSC Adv* 2015;5:44587–97.
- [29] Yuphintharakun N, Nurerk P, Chullasat K, Kanatharana P, Davis F, Sooksawat D, et al. A nanocomposite optosensor containing carboxylic functionalized multiwall carbon nanotubes and quantum dots incorporated into a molecularly imprinted polymer for highly selective and sensitive detection of ciprofloxacin. *Spectrochim Acta A Mol Biomol Spectrosc* 2018;201:382–91.

SUPPLEMENTARY FIGURES

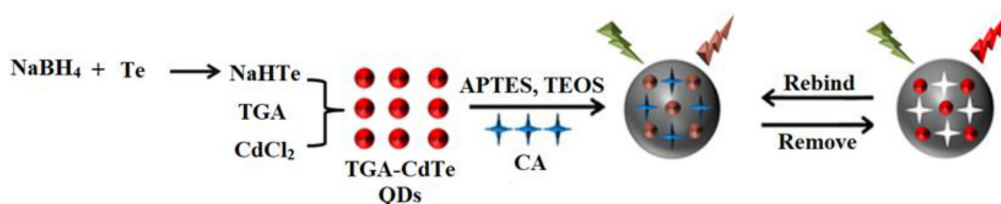


Figure S1 | Schematic illustration of the synthesis of CdTe-QDs@MIPs. QD, quantum dot; MIP, molecularly imprinted polymer.

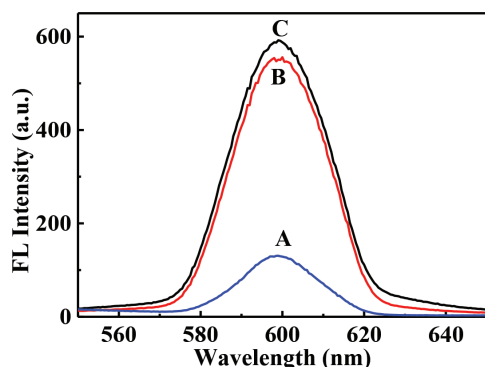


Figure S2 | Fluorescence spectra of CdTe-QDs@MIPs before (A) and after (B) removal of CA, and fluorescence spectra of CdTe-QDs@NIPs (C). Qd, quantum dot; MIP, molecularly imprinted polymer; NIP, non-imprinted polymer; CA, caffeic acid.

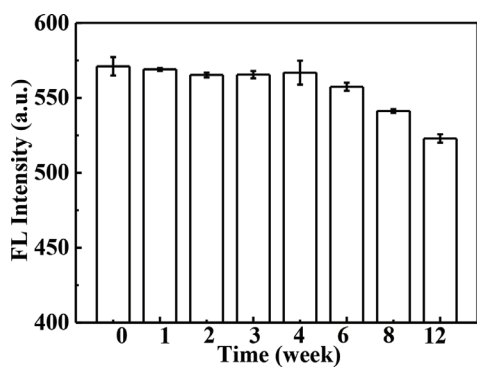


Figure S3 | Effect of store time on the response of CdTe-QDs@MIPs. QD, quantum dot; MIP, molecularly imprinted polymer.

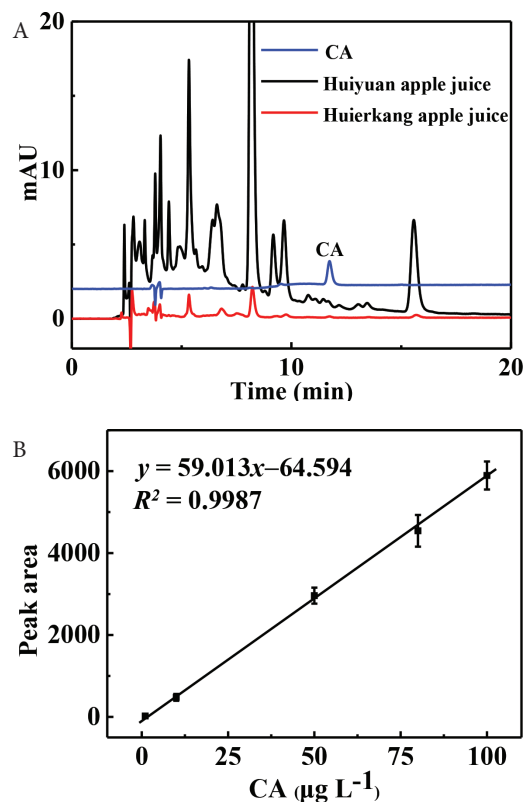


Figure S4 | HPLC chromatograms of CA, Huiyuan apple juice and Huierkang apple juice (A), and the calibration graph (B). HPLC, high-performance liquid chromatography; CA, caffeic acid.